

DISCUSSION OF H.V. POWER SUPPLY UNITS CONNECTED
WITH HIGH GRADIENT TUBES IN LINAC PREINJECTORS*

V.J. Kovarik and Th.J.M. Sluyters
Brookhaven National Laboratory
Upton, L.I., New York

Introduction

In the new accelerating tubes of preinjectors, the gradients (30-50 kV/cm) are significantly larger than in conventional tubes (5-10 kV/cm). The electrons, extracted from the metal surfaces inside the vacuum by electric field emission, increase rapidly with the field strength. A sudden large increase of current, known as a vacuum breakdown or discharge, damages the electrodes, thereby triggering other breakdowns. In the arrangement of high voltage power supplies for high gradient tubes, it is essential to reduce the current in such a discharge. This can be realized by a surge resistor in series with a reduced filter capacitor. However, this influences the beam loading characteristics and consequently the circuit (called the "bouncer") that compensates for it.

In the first section, the selection of the surge resistor in an open 750 kV circuit and its consequences in possible "bouncer" systems are discussed.

In the second section, the characteristics of the 850 kV Haefely Cockcroft-Walton are discussed.

Section I

A. The Choice of the Surge or Protective Resistor

As is mentioned in the introduction, the electron current, extracted from cold surfaces, increases rapidly with field strength. The transition of the field emission into the breakdown state, which can be caused by many types of mechanisms (Ref. 1), has a much larger probability of occurring at higher field gradients. The existence of secondary electrons in a high gradient tube is demonstrated in the melting of metal inside the downstream side of the shielded expansion cup without the ion source in operation. (See Fig. 1). The acceleration geometry probably helps to focus the field emitted electrons back into the cup. This phenomenon does not occur in low gradient machines.

A less dramatic demonstration of the cold field emission is the voltage drop on the high voltage terminal detected by a capacitive pickup system. (See Fig. 2). The micro-discharges,

appearing in pairs and separated about 200 μ sec do not in general cause complete breakdown of the column; this depends on the "damage" of the anode and the electrical strength of the gap. The "damage" of the electrodes depends on the current flow into the discharge. In the appendix, the micro-discharges are discussed in somewhat more detail (as far as we understand them!) Figure 3 shows the decrease of discharge current flow and complete voltage breakdowns with increased surge resistor. In an experiment, the column was conditioned with a high protective resistor (400 k Ω);[‡] the resistor was then replaced for lower values, 140 k Ω and 40 k Ω . With 40 k Ω , the column was damaged to the point where it was impossible to maintain the conditioned voltage and at least 140 k Ω had to be put back in the circuit.

From these measurements, we can conclude a minimum series resistor of 140 to 400 k Ω .^{**} The consequences of this resistor in the H.V. circuit are discussed in the next paragraph.

B. H.V. Circuits for High Gradient Tubes

The basic electrical circuit of the open high voltage structure of the operational machine as well as in the test area is shown in Fig. 4.

Figure 5 is the theoretical voltage droop for a 250 mA beam current as a function of time. The experiments show voltage drops, which are about 20% larger than the theoretical values, caused by pulse backstreaming electrons. In Van de Graaff machines and low gradient accelerating tubes, a much higher ratio is found in general. A possible explanation is the short path length (\sim 1 cm) in the effective ionization energy range ($<$ 50 keV) in the high gradient tubes.

In order to reduce the voltage drop to less than 750 volts ($<$ 0.1%) a bouncer system must be incorporated and able to supply a $\Delta V = I(R + \Delta t/C_2) = 107.5$ kV. (See Fig. 6).

In the scheme of Fig. 6, the bouncer system is coupled to the high voltage terminal through a high impedance (large protective resistor in series with a large coupling capacitance). A smaller coupling capacitance could not be tried

[‡]Conditioning times vary from three hours to three days depending on the previous history of the column.

^{**}It might be possible that a lower filter or coupling capacitance allows a lower value.

*Work performed under the auspices of U.S. Atomic Energy Commission.

out to study its effect on column damage.

Note: The leakage reactance of a transformer may be used as a high impedance. (See Fig. 7). This method has the advantage of allowing bouncer tubes to work in a lower voltage and high current range. If the early part of the beam can be chopped off and with reasonably stable intensity, bandwidth requirements are not difficult to realize (1 kc - 30 kc).

Three "bouncer" solutions are considered:

1. Spark gap feedback.
2. Series hard tube modulator.
3. Combination spark gap and shunt hard tube feedback.

1. Spark Gap Feedback

Figure 8 shows the basic spark gap scheme. As mentioned above, the drive voltage needed and stored on the H.V. condenser is 107.5 kV.

The advantage of this scheme is its simplicity and the accelerating tube is protected by an effectively higher resistor. In practice, the source current is very stable and constant in intensity. This solution seems to be an adequate substitute in case of breakdown of the hard tube modulator feedback system. An example of the spark gap bouncer beam compensation is shown in Fig. 9.

2. Hard Tube Modulator

Figure 10 shows a basic schematic of a conventional series hard tube modulator.

This system has two disadvantages:

1) The large dynamic range required ($\Delta V \approx 107.5$ kV) has to be supplied by the modulator tube.

2) Voltage variations on the high voltage terminal are always in the closed servo loop. This provides a low impedance source of current for the micro-discharges.

These disadvantages can be overcome by transformer coupling (lower ΔV required by the modulator tube) and by switching the servo loop on only during the beam pulse.

3. Combination Spark Gap and Shunt Hard Tube Modulator

In this combination scheme, the major droop would be taken care of by the spark gap and smaller changes adjusted by the modulator. (See Fig. 11).

This system has the following advantages:

1) Being completely decoupled between beam pulses.

2) A lower servo loop gain since the major droop is taken care of by the spark gaps.

3) Larger column protection by virtually increasing the column series resistance.

Figure 12 is an example of beam compensation using the combined spark gap and modulator scheme.

Section II

Discussion of the Haefely Power Supply (850 kV)

Some pertinent parameters of the Haefely generator are:

Stability	- ± 375 V @ 750 kV
Dc current	- 12 mA continuous
Beam current	- 0.5 A for 100 μ sec (max.)
Pulse rate	- 10 pulses per sec.
Meas. equip.	- compensated divider and associated electronics shall not contribute more than ± 75 V of error in the measurement of the high voltage during the beam pulse.

Figure 13 is the basic system that will be provided by Haefely.

The stray capacitance is assumed to be 400 pF. The compensated divider will increase the capacity of the high voltage terminal to 800 pF. It is not known if the high gradient column can stand this factor of two increase without damage to the electrodes. In the event that this will not work, the capacitors will have to be removed and a plate will have to be mounted on the side wall of the pit. This will form a capacitive divider that provides a signal for the bouncer. This technique has been applied successfully in our test area. The compensated divider will be mounted on the side of the high voltage terminal as shown in Fig. 14. This method of mounting will minimize the undesirable coupling between the compensated divider and the bouncer coupling. The bouncer is coupled to the high voltage terminal by three stacks as shown in Fig. 15.

The surge resistors (R in Fig. 15) are removable so that they can be changed if necessary.

D_1, D_2, D_3, D_4 can be removed so that some capacity can be added. This allows some lead compensation to be introduced in the coupling scheme.

The use of three coupling stacks will provide the system with the necessary flexibility and allow any of the basic methods previously described to be incorporated.

In the described Haefely circuit the voltage drop using formula (1) is:

$\Delta V \approx 20$ kV for 250 mA beam current
 $(C_1 = 800$ pF $C_2 = 1500$ pF $R = 70$ k Ω $t = 100$ μ sec)
 and $\Delta V \approx 40$ kV for 500 mA beam current. The
 Haefely driver requirements for the bouncer
 system are respectively 34 and 68 kV. The required
 bandwidth of the bouncer system can be estimated
 by considering the stability requirements. These
 estimates are listed in Table I. (See also Fig. 3).
 Reduction of the bandwidth requirement can be
 accomplished by a program system that produces the
 required V_1 . Both gain and bandwidth requirements
 can be lowered in this way. The combination spark
 gap and shunt regulator is an example of this
 method. In case that the capacity of the voltage
 divider has to be removed to reduce damage to the
 accelerating electrodes, the bandwidth requirements
 for a linear servo loop are more severe than in
 the previous case. The frequency response should
 be $f = 0.34/3.12 \times 10^7 \approx 1$ Mc.

Appendix

Micro-Discharges

During initial column conditioning, the
 micro-discharges occur at a rate of one to two
 per second, and drop off to approximately five to
 ten per hour after conditioning. This implies,
 that during conditioning, the bouncer should not
 be connected due to greater probability of causing
 damage to the column. After conditioning, the
 bouncer should only be connected during the beam
 pulse.

Figure 2, in Section I, shows the voltage
 drop on the H.V. terminal due to a micro-discharge
 (in general smaller than 20 kV) and Fig. 3 the
 decrease of relative current flow in such a dis-
 charge with increased series resistor. The micro-
 discharges between the high gradient electrodes
 occur mostly in pairs with dV/dt significantly
 larger in the initial discharge. (See Fig. 17).

From Fig. 2 let us estimate the current flow
 (I_1) , which is determined by the voltage drop
 across the electrodes and the stray capacitance
 made up of (see Fig. 18):

- a) the terminal capacitance $C_1 \approx 400$ pF.
- b) the capacitance between the high
 gradient electrodes $C_2 \approx 200$ pF.
- c) the capacitance between the voltage
 divider rings $C_3 \approx 130$ pF.

The equivalent of Fig. 18 is shown in Fig. 19.
 When the micro-discharges take place between any
 pair of high gradient electrodes the equivalent
 circuit is as shown in Fig. 20, in which
 $\frac{C_3 + C_2/3}{4} = 50$ pF and $\frac{dV_e}{dt}$ is the voltage change
 across two high gradient electrodes:

$$\frac{dV_e}{dt} = \frac{dV}{dt} \frac{C_1 + \frac{C_3 + C_2/3}{4}}{\frac{C_3 + C_2/3}{4}} \approx$$

$$\frac{10 \times 10^3}{4 \times 10^{-6}} \frac{400 + 50}{50} = 22.5 \times 10^9$$

and so the mean discharge current (I_1) is given
 by:

$$i = \left\{ \frac{C_3 + C_2/3}{4} + (C_3 + C_2/3) \right\}$$

$$\frac{dV_e}{dt} = 250 \times 10^{-12} \times 22.5 \times 10^9 \approx 5.6$$
 A

This indicates that almost complete breakdown
 occurs between the electrodes during a micro-
 discharge since:

$$\int_0^V dV_e = 22.5 \times 10^9 \int_0^{4 \times 10^{-6}} de \approx 90$$
 kV

The terminal voltage drop is approximately
 10 kV, therefore, 80 kV has to be distributed
 among the other electrodes (≈ 20 kV/gap). This
 assumes identical gap capacities. Unequal
 capacities could cause complete column breakdown.
 The secondary burst (I_2) can be approximated in
 the same manner. From Fig. 2 the magnitude is
 approximately 0.3A with V_e reading approximately
 115 kV. The decay in Fig. 2 is the time constant
 of the surge resistor charging up the stray
 capacity ($\approx 2 \times 10^{-4}$ sec.). Complete column
 breakdown (when triggered by micro-discharges)
 occurs in time anywhere between the start of the
 initial discharge and the end of the secondary
 discharge. There seems to be no indication of
 complete breakdown dependence on the initial
 burst or secondary burst.

Conclusions

- 1) Low terminal capacity is desirable.
- 2) Beam servo loop on only during pulse.
- 3) Individual gaps have to stand a 10 to 20%
 increase in voltage for short periods.
- 4) Gap capacity should be uniform.

In addition to the above it may be possible
 to isolate each accelerating gap by a resistor.
 This would limit the micro-discharge current and
 also invalidate conditions 1) and 2).

References

1. A.S. Denholm, "The Electrical Breakdown of Small Gaps in Vacuum," Can. J. Phys. 36, 476 (1958).

Table I - Required bandwidth for 250 and 500 mA pulsed proton beams of 100 μ sec.

Beam Current	$\frac{\Delta V}{\Delta t} = a$	ΔV (Volts)	$\Delta t = \frac{\Delta V}{a}$	Frequency Response $\frac{0.34}{\Delta t}$
250 mA	3×10^8	375	12.5×10^{-7}	270 kc
500 mA	6×10^8	375	25×10^{-7}	540 kc

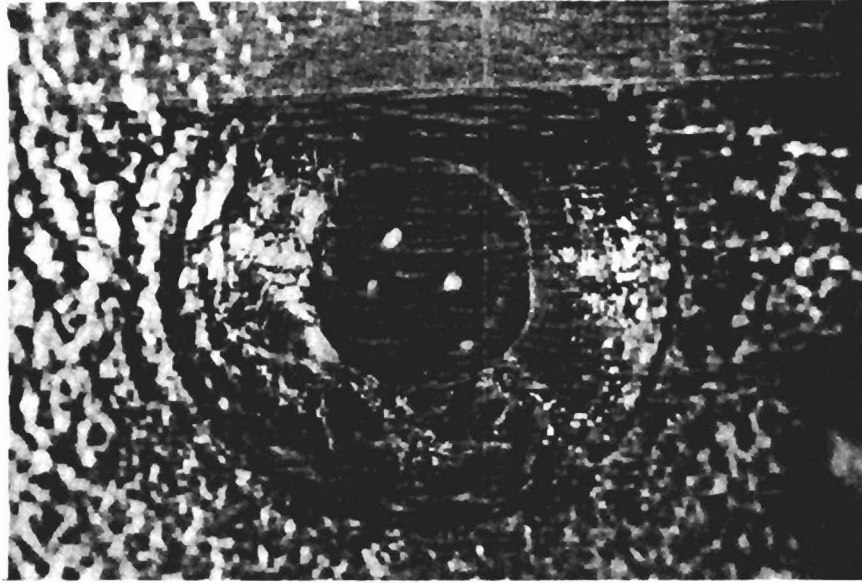


Fig. 1a - Craters around a mild steel anode aperture of the expansion cup, caused by field emission electrons (10 X).

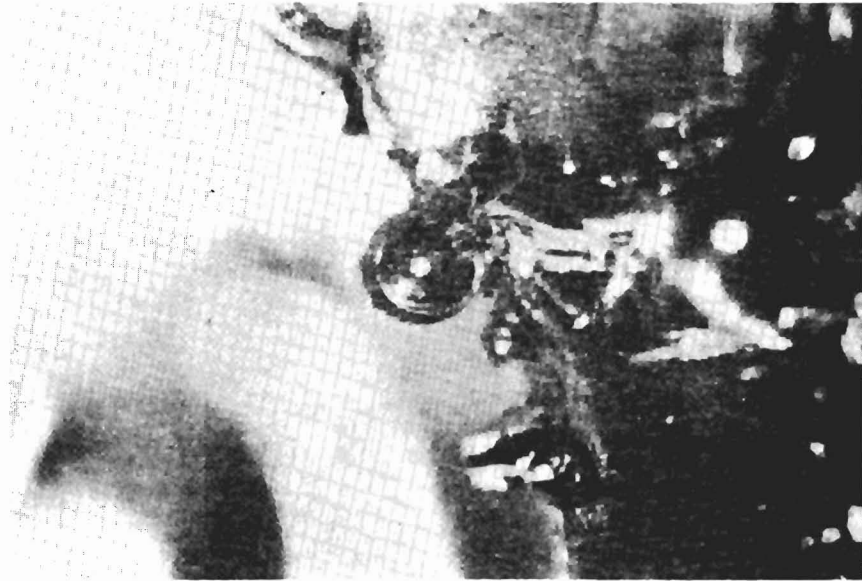
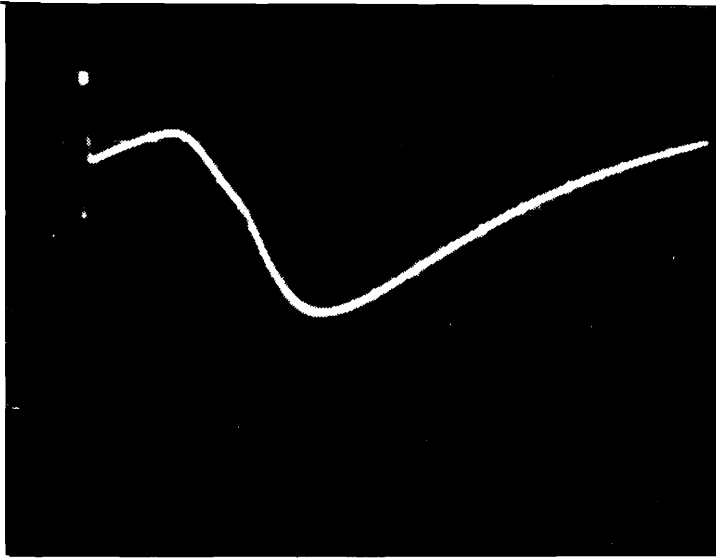


Fig. 1b - A 100 X enlargement.



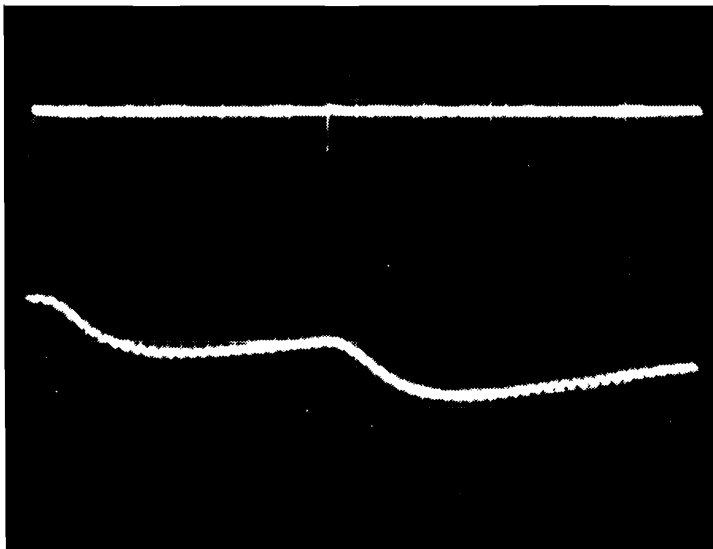
Top Trace:

Ampl. 7.5 kV/cm
Sweep 50 μ sec/cm

Bottom Trace:

Ampl. 3.75 kV/cm
Sweep 2 μ sec/cm

Fig. 2a - A typical micro-discharge as they appear on the capacitive pickup plate.



H. V. Trace:

Sweep 0.1 sec/cm

Pressure Trace:

————— 3×10^{-6} mm Hg
————— 5×10^{-6} mm Hg

Fig. 2b - Micro-discharges as they appear on the H. V. and vacuum traces.

Relative
Current
flow into
micro-discharges

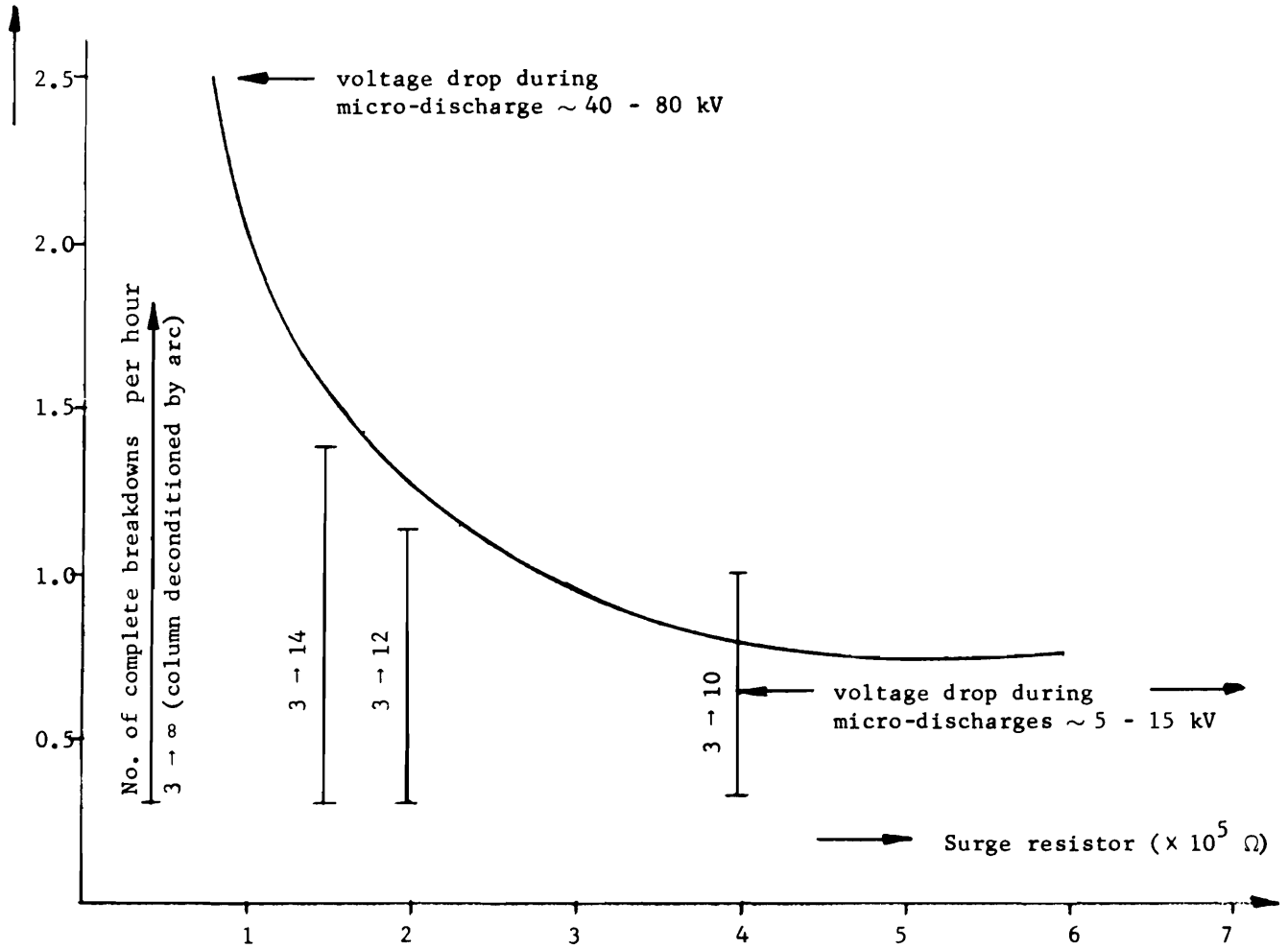


Fig. 3 - The decrease of discharge current flow and complete voltage breakdowns by increased surge resistor.

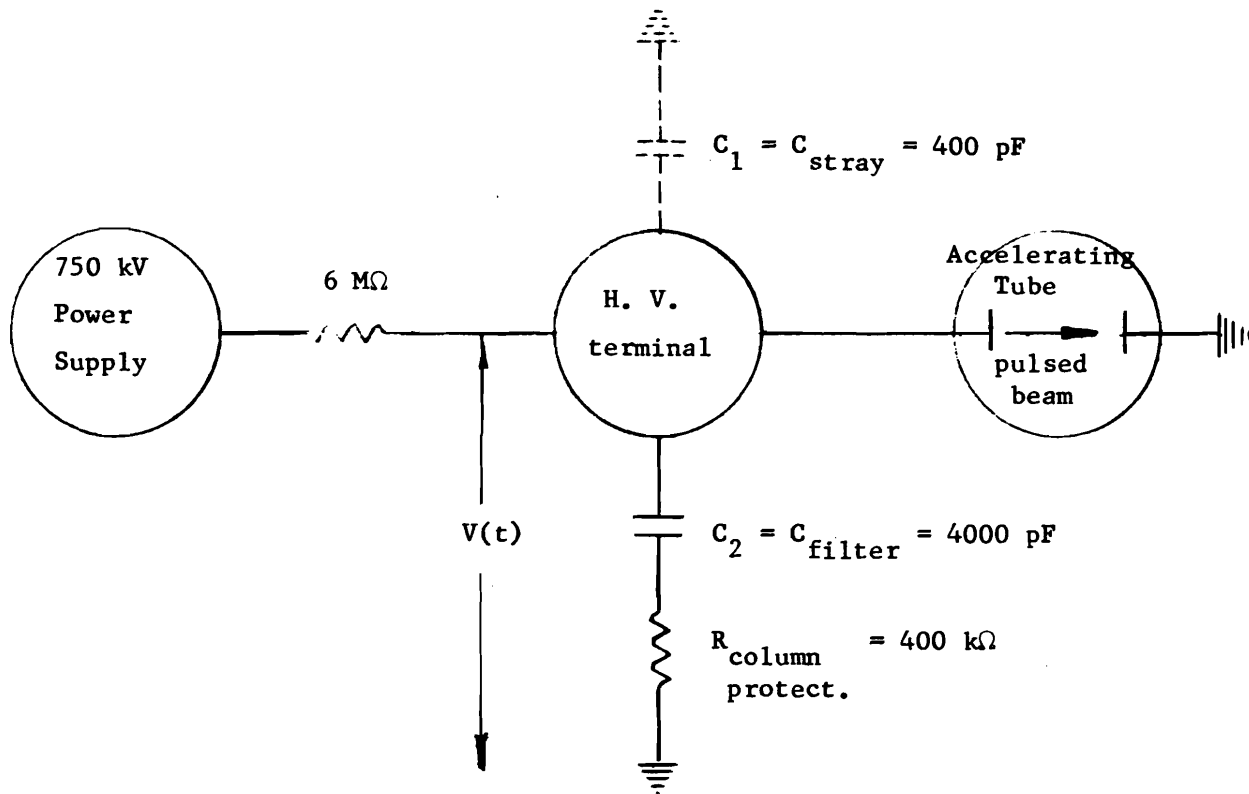


Fig. 4 - Basic scheme of the open high voltage structure.

The voltage drop $\Delta V(t)$ during the beam pulse is:

$$\Delta V(t) = - \frac{I}{C_1 + C_2} \left[\Delta t + \frac{C_2^2 R}{C_1 + C_2} \left(1 - e^{-\left[\frac{(C_1 + C_2)}{C_1 C_2 R} \right] \Delta t} \right) \right] \quad (1)$$

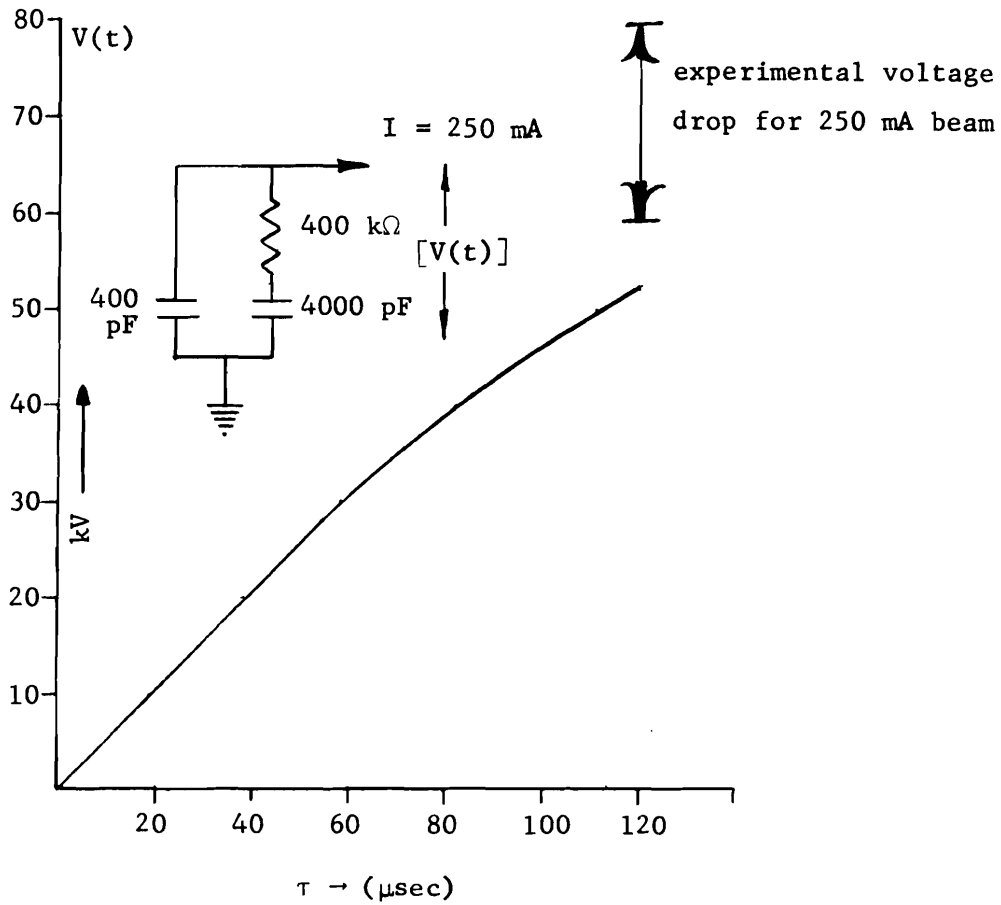


Fig. 5 - Voltage drop for a 250 mA pulsed beam as in the structure mentioned above.

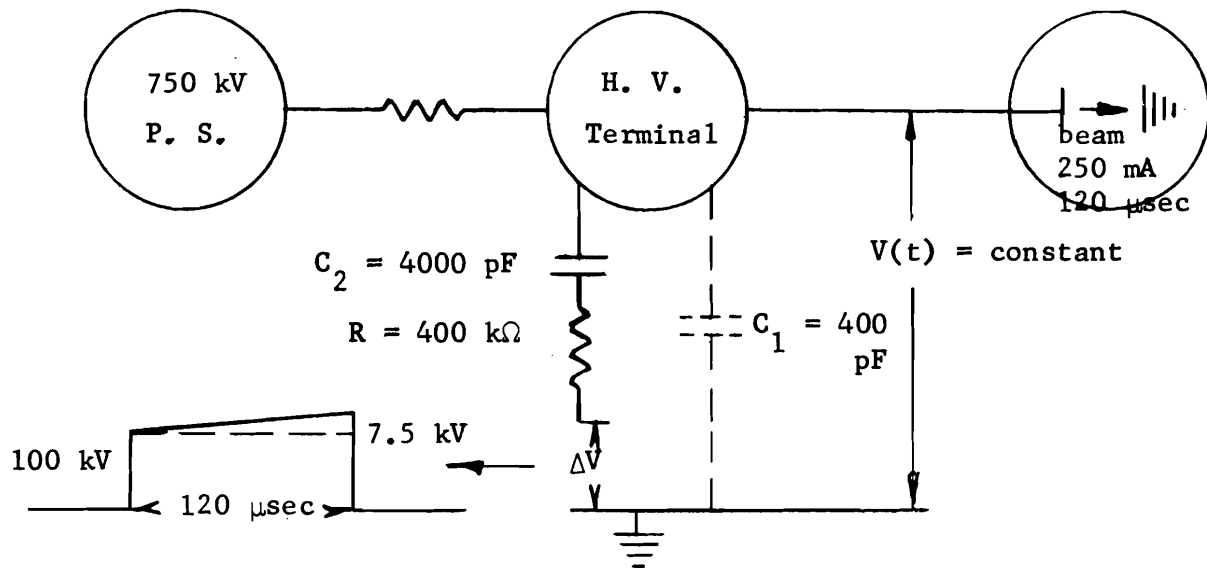


Fig. 6 - In this scheme 107.5 kV is necessary to compensate for a total 63 kV terminal drop without compensation.

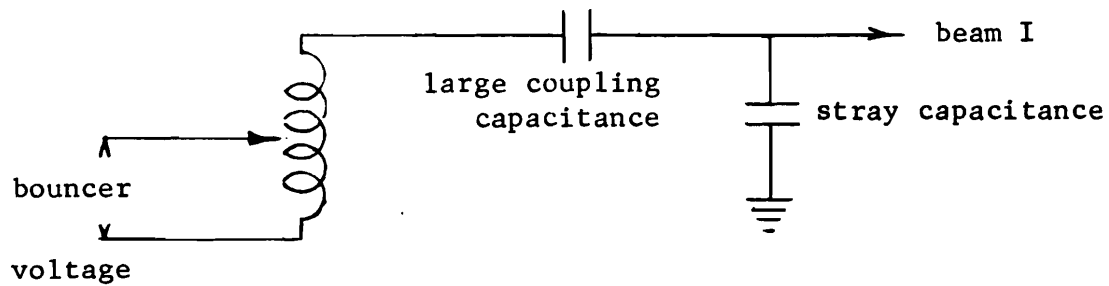


Fig. 7 - A possible bouncer arrangement.

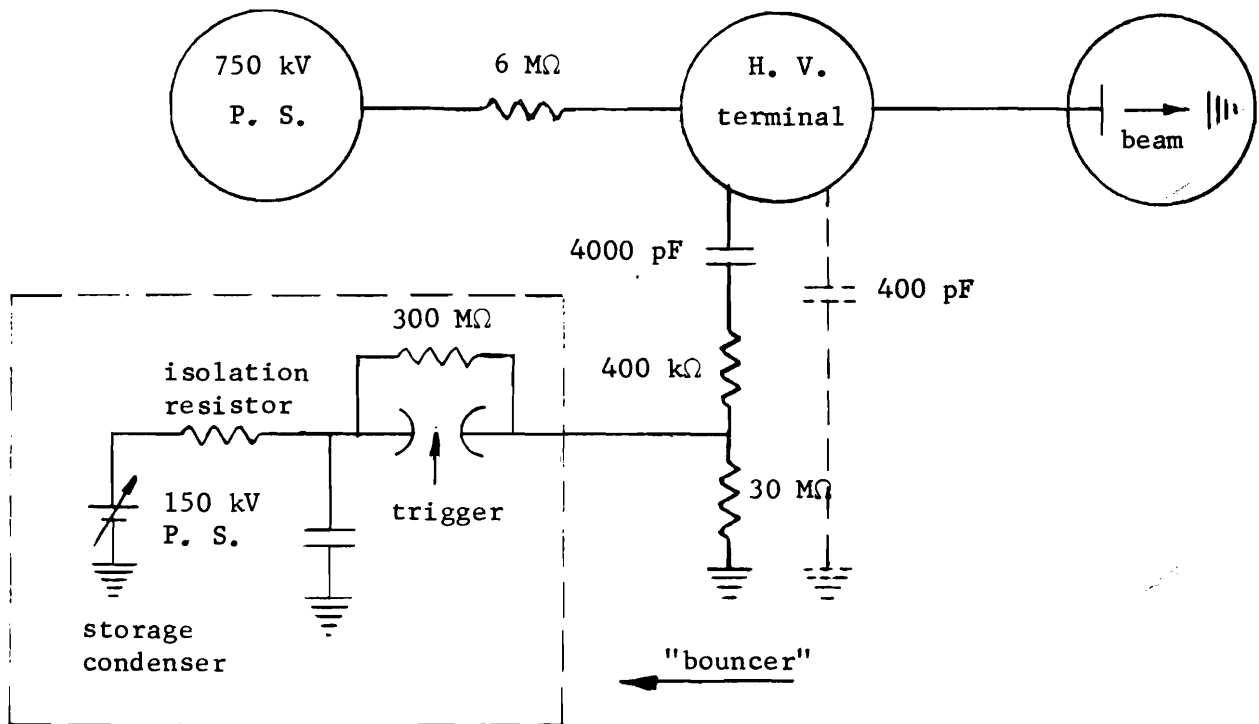


Fig. 8 - Spark gap "bouncer" system.

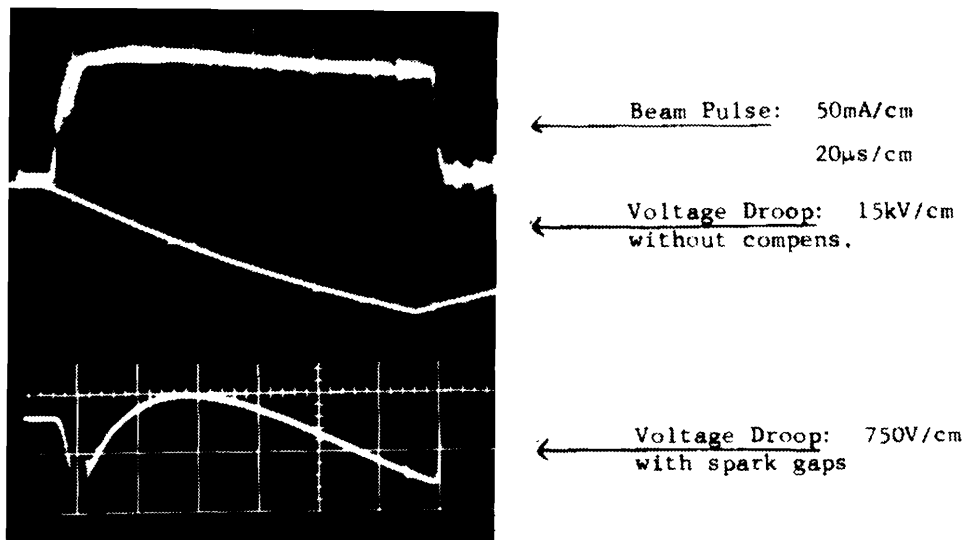


Fig. 9 - Demonstration of beam loading and spark gap compensation for a 100 mA beam current in the 750 kV high gradient accelerator.

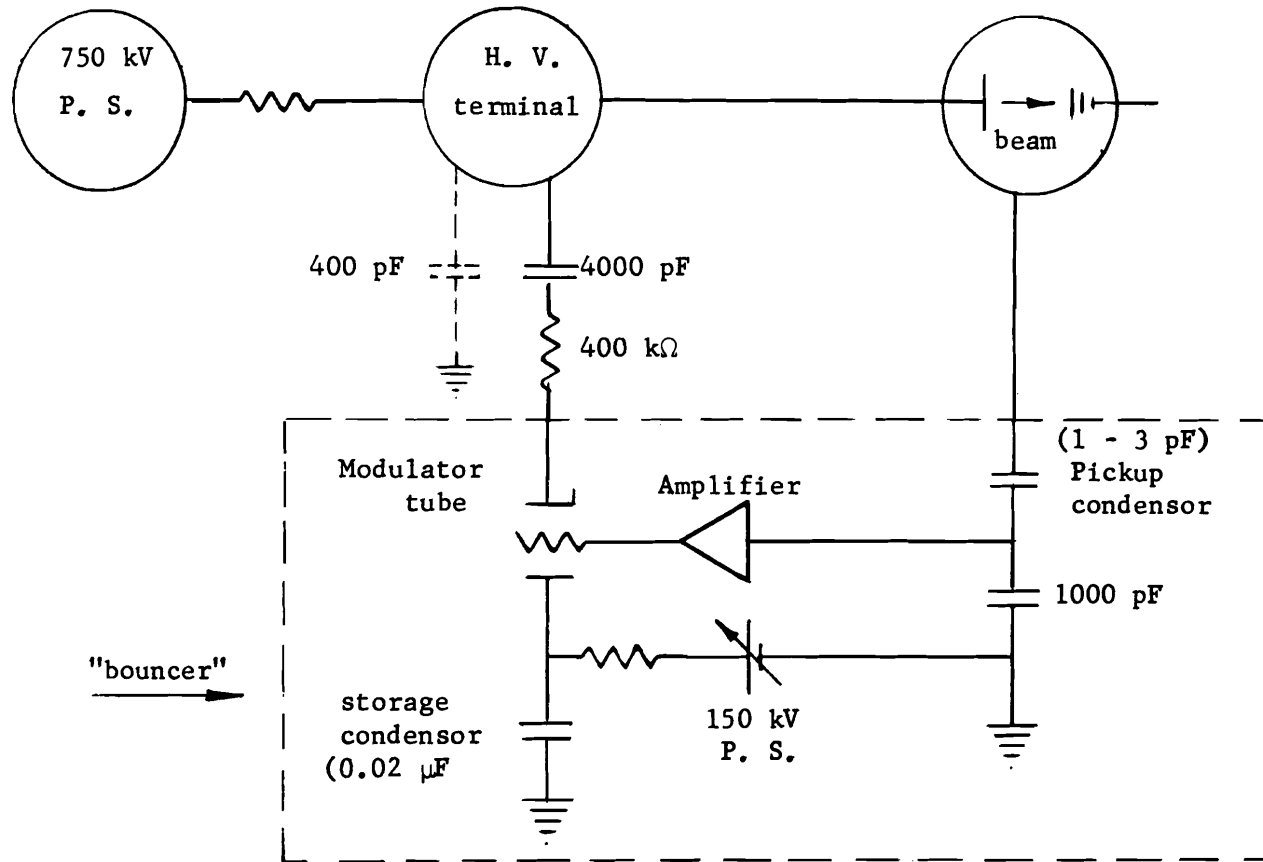


Fig. 10 - Conventional series hard tube modulator "bouncer" system.

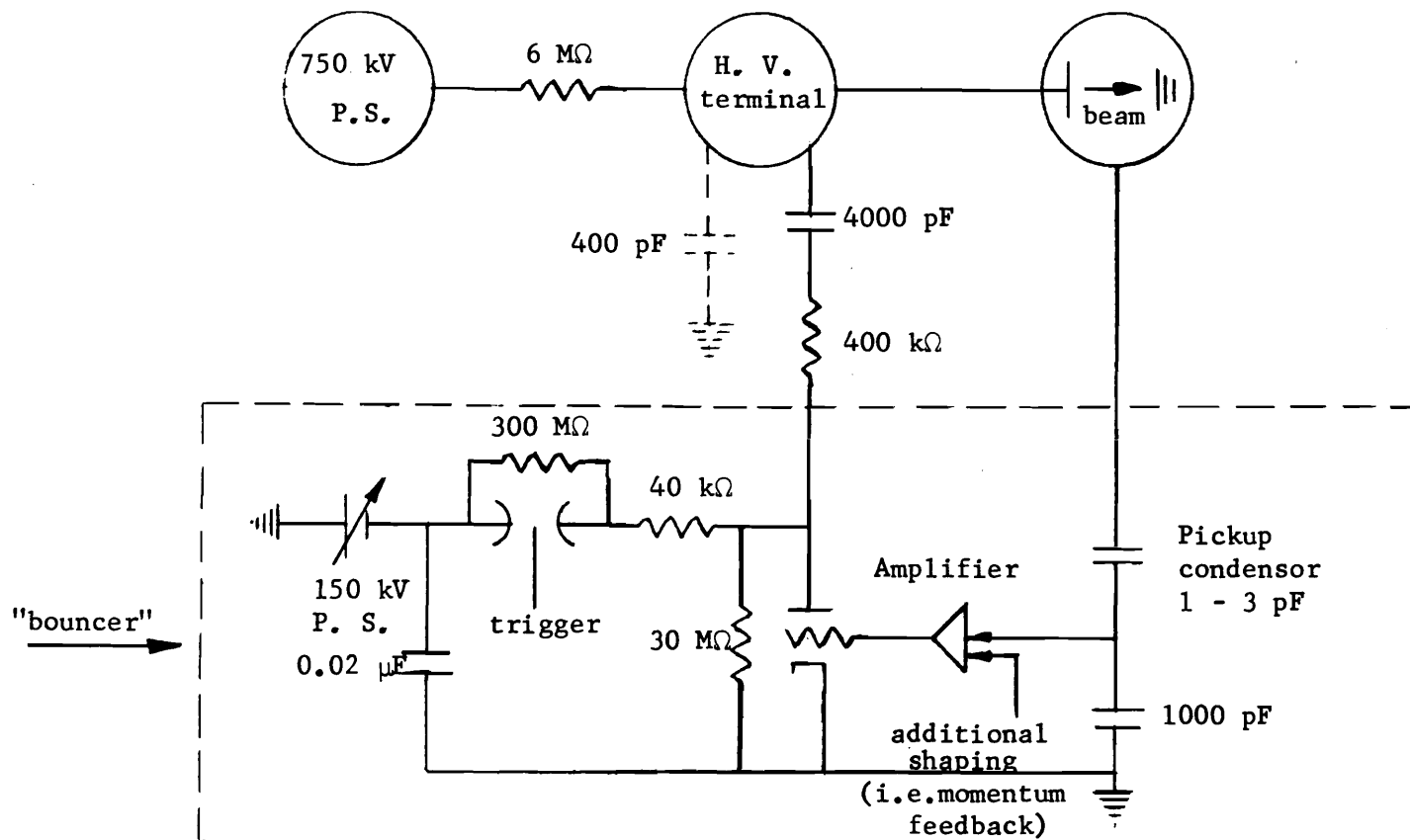


Fig. 11 - Combination spark gap and hard tube modulator.

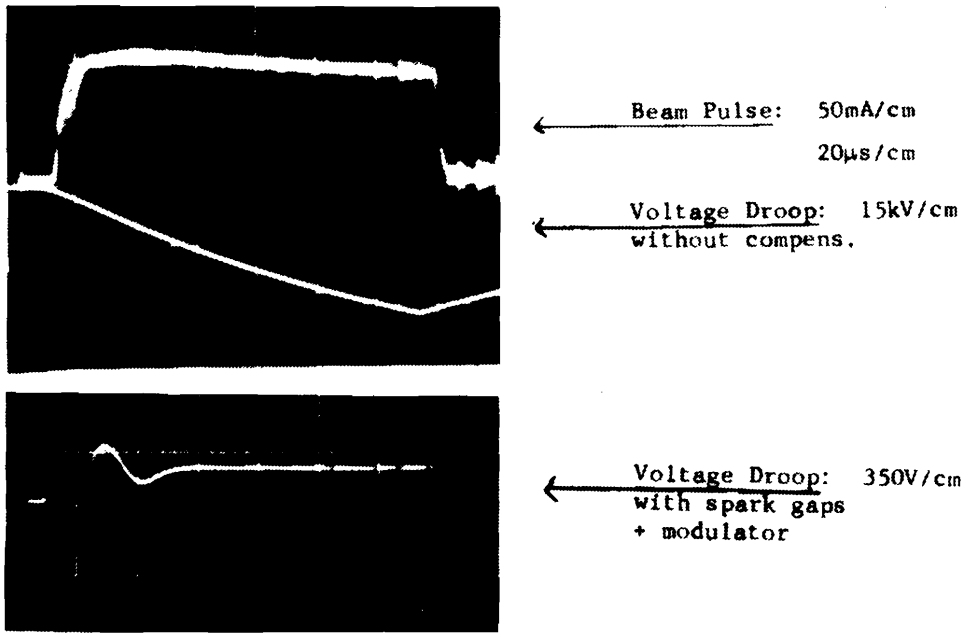


Fig. 12 - Demonstration of beam loading compensation for a 100 mA beam in the 750 kV high gradient accelerator, using the combined spark gap and modulator bouncer.

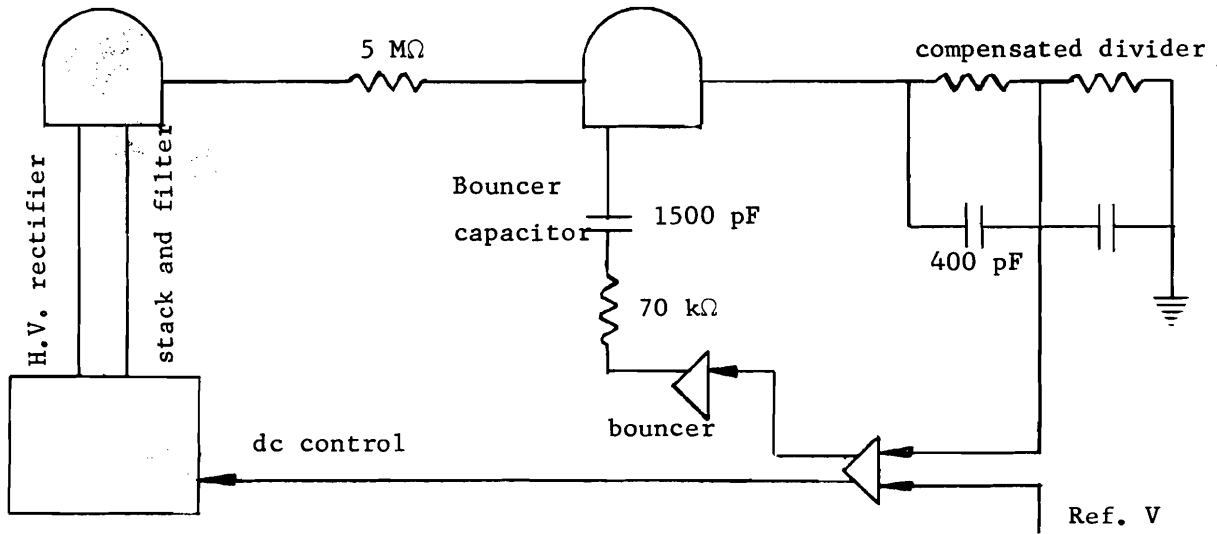


Fig. 13 - Schematic of the high voltage power supply and related equipment.

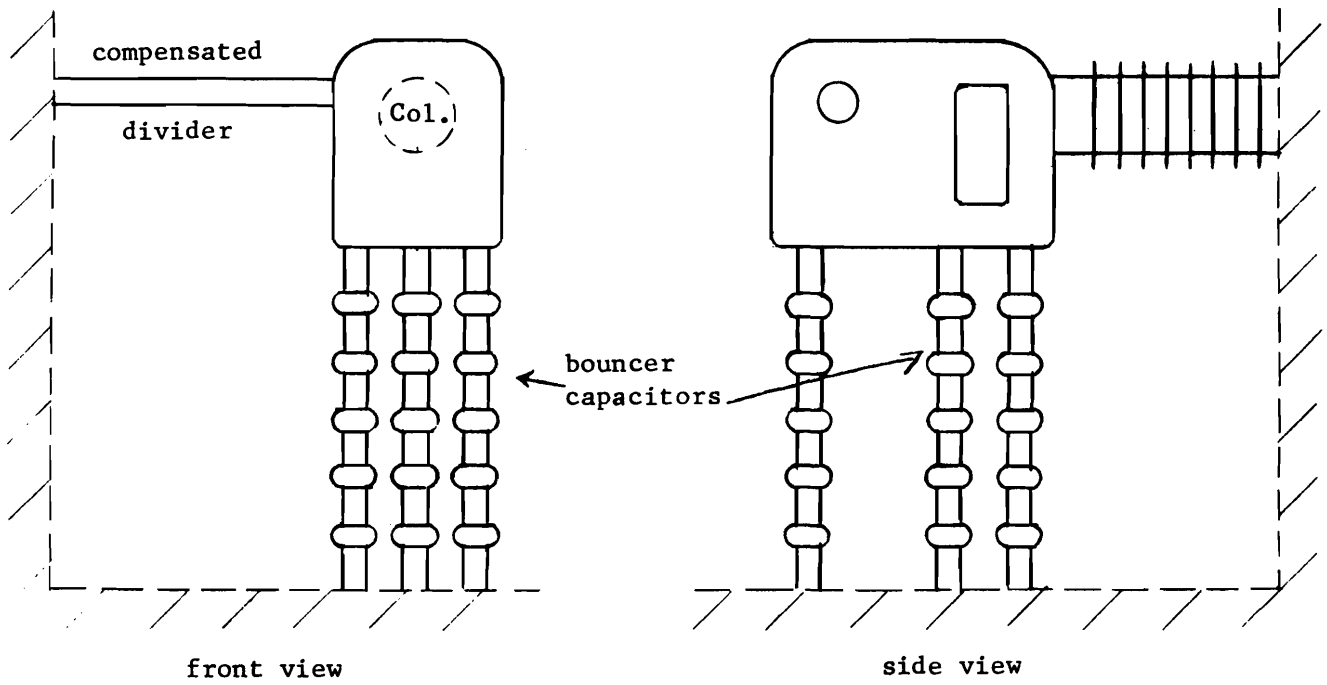


Fig. 14 - Arrangement of high voltage terminal, accelerating column, divider and filter stack.

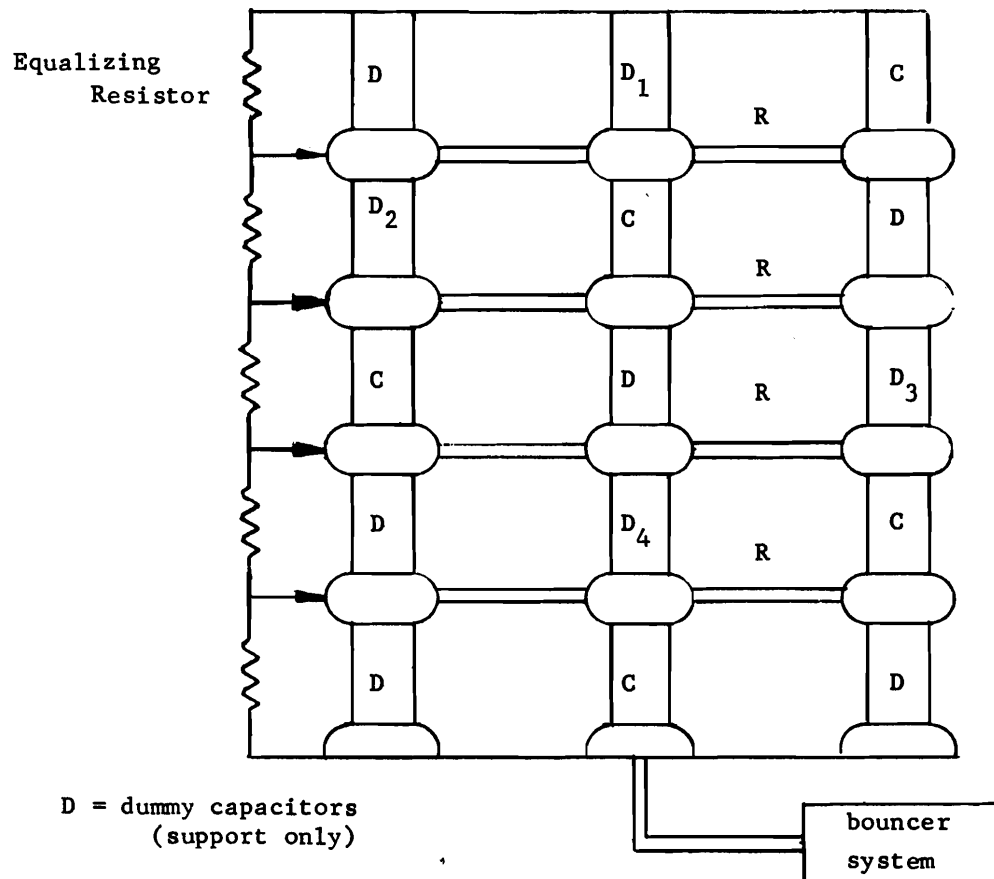


Fig. 15 - Schematic of filter stack.

$$\left\{ \Delta V_i = I \left(R + \frac{t}{C} \right) \right\}$$

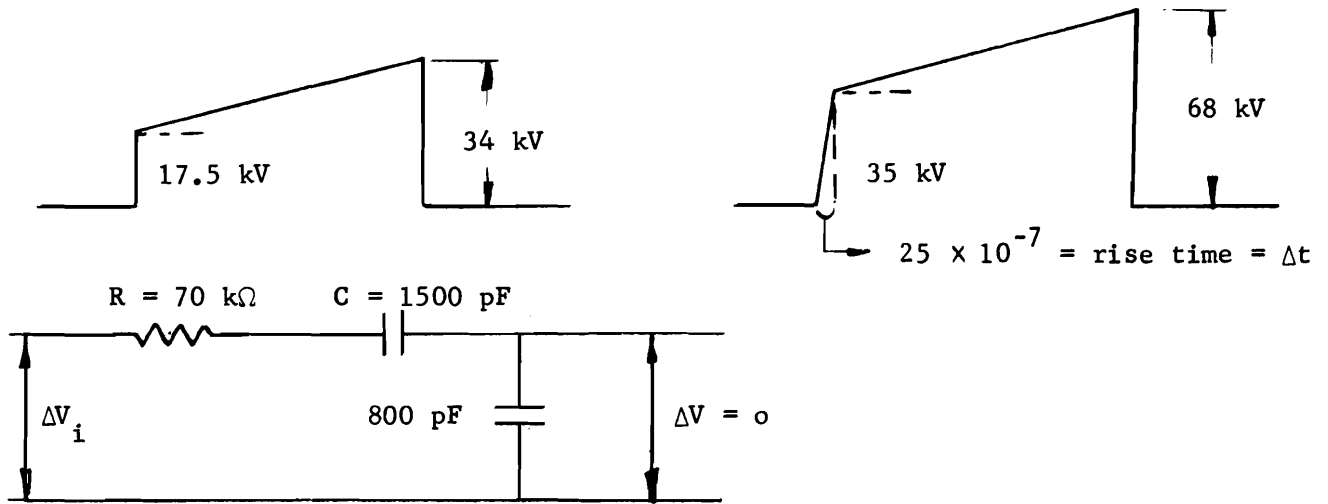


Fig. 16 - The equivalent Haefely diagram and driver requirements for resp. 250 and 500 mA beams.

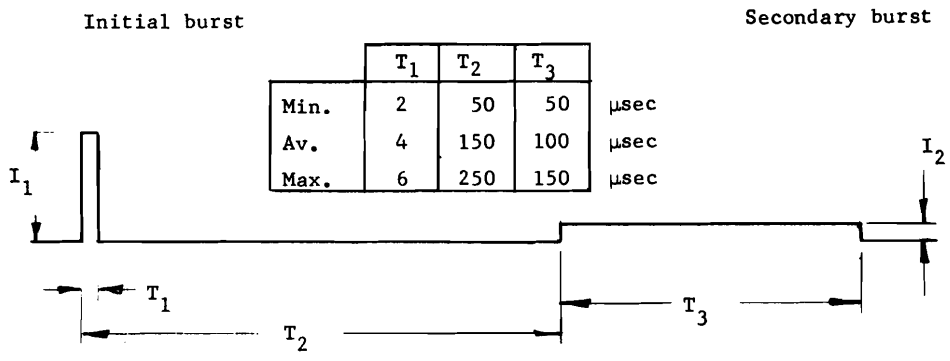


Fig. 17 - Typical time sequences of the microdischarges.

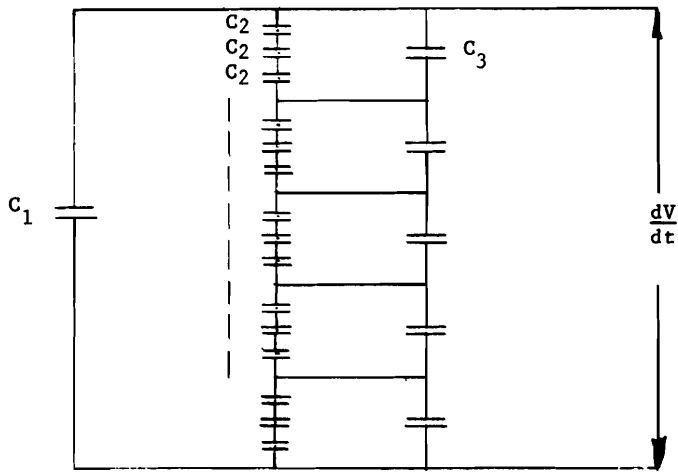


Fig. 18 - Capacitances connected with the accelerating tube.

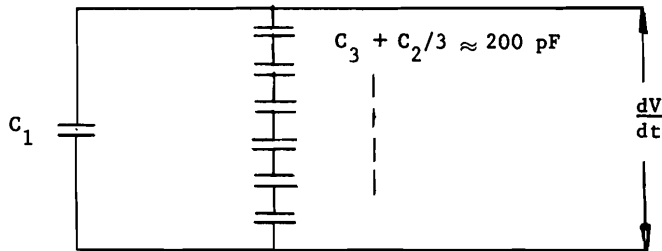


Fig. 19 - Equivalent circuit of figure 18.

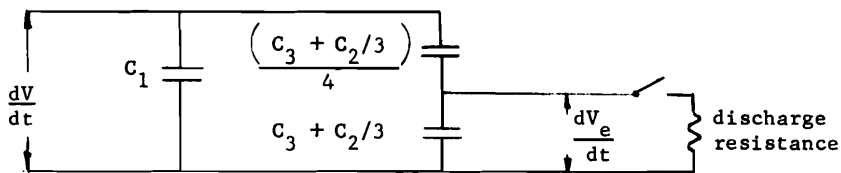


Fig. 20 - The equivalent circuit of Fig. 19 in case of a discharge between a pair of electrodes.